LASER INTERFEROMETER GRAVITATIONAL WAVE OBSERVATORY
- LIGO -
CALIFORNIA INSTITUTE OF TECHNOLOGY
MASSACHUSETTS INSTITUTE OF TECHNOLOGY

Technical Note **LIGO-T1800296–v1** 2018/06/25

Constructing a Homodyne Detector for Low Quantum Noise Gravitational Wave Interferometry

SURF Student: John Martyn
Mentors: Kevin Kuns, Aaron Markowitz, Andrew Wade, Rana Adhikari

California Institute of Technology
LIGO Project, MS 18-34
Pasadena, CA 91125
Phone (626) 395-2129
Fax (626) 304-9834
E-mail: info@ligo.caltech.edu

Massachusetts Institute of Technology
LIGO Project, Room NW22-295
Cambridge, MA 02139
Phone (617) 253-4824
Fax (617) 253-7014
E-mail: info@ligo.mit.edu

LIGO Hanford Observatory
Route 10, Mile Marker 2
Richland, WA 99352
Phone (509) 372-8106
Fax (509) 372-8137
E-mail: info@ligo.caltech.edu

LIGO Livingston Observatory
19100 LIGO Lane
Livingston, LA 70754
Phone (225) 686-3100
Fax (225) 686-7189
E-mail: info@ligo.caltech.edu

http://www.ligo.caltech.edu/

1 Introduction and Background

Achieving more efficient detection of gravitational radiation is a goal of contemporary experimental physics, as it will enable novel tests of general relativity and provide information on astronomical bodies that are difficult to observe through the electromagnetic spectrum. The gravitational waves (GWs) that encompass this radiation are described by oscillatory perturbations to a background spacetime metric. These waves manifest themselves physically by altering displacements in spacetime, such as spatial distances and time durations. Current GW observatories, such as LIGO, use high precision laser interferometry to detect miniscule changes in the length of interferometer arms, indicating the passage of a GW. Since typical changes in the LIGO arm lengths induced by GWs are of the order of 10^{-18} m, incredibly precise measurements must be conducted to observe a GW. In particular, LIGO uses a large Michelson interferometer furnished with Fabry-Perot cavities and power recycling mirrors to optimize its sensitivity and ability to detect GWs.

Despite their intricate designs, interferometric GW detectors are subject to various sources of noise that limit their resolution. Some of this noise arises from external sources, like human activity and weather patterns. The resulting noise can be combated by numerous techniques, such as performing interferometry in vacuum chambers and employing vibration isolation systems. Furthermore, on atomic and subatomic scales, new sources of intrinsic noise arise as the laws of quantum mechanics take precedence over those of classical physics. For instance, in quantum electrodynamics (QED), the quantized electromagnetic field reveals the discrete photon nature of light. This phenomenon introduces shot noise and radiation pressure noise into the interferometer due to the fact that the electromagnetic field of a beam of light is not smooth and continuous, but rather is composed of individual photons. Noise that arises from quantum mechanical processes is known as quantum noise and owes its existence to the Heisenberg uncertainty principle and quantum fluctuations. Because of these immutable laws, sources of quantum noise dictate that the sensitivity of classical GW interferometers is bounded below by the Standard Quantum Limit (SQL). For example, in a GW interferometer with arm lengths L, test masses of mass m, and detecting a GW of frequency Ω, the noise spectral density of the GW strain, h, is bounded below by [5]

$$S_h^{\mathrm{SQL}}(\Omega) = \frac{2\hbar}{m\Omega^2 L^2}. \tag{1}$$

In general, the SQL will differ depending on the precise interferometric setup, but the limitations it conveys remain the same.

However, it turns out that the SQL only applies to interferometers when the sources of noise are uncorrelated, as they are classically. In fact, despite its counterintuitive name, the SQL can be surpassed by cleverly constructed interferometers that take into account quantum mechanics and correlated noise. One such method of beating the SQL involves squeezed light and balanced homodyne detection, incorporating various aspects of quantum mechanics and QED. In QED, the electric field of a beam of light can be described by amplitude and phase quadrature operators, $\hat{X}_1$ and $\hat{X}_2$, respectively. Explicitly, the electric field of freely propagating monochromatic light with amplitude E_0, angular frequency ω, and polarization $\mathbf{p}(\mathbf{r}, t)$, can be expressed as [10]

$$\hat{\mathbf{E}}(\mathbf{r}, t) = E_0(\hat{X}_1 \cos(\omega t) - \hat{X}_2 \sin(\omega t))\mathbf{p}(\mathbf{r}, t). \tag{2}$$

By the canonical commutation relations of QED, the quadrature operators do not commute: $[\hat{X}_1, \hat{X}_2] \neq 0$. Hence, they obey an uncertainty principle, wherein the product of their standard deviations, or uncertainties, cannot decrease below 1. Since the quantum state of a beam of light can be expressed in terms of these operators, as in Eq. (2), this necessarily introduces uncertainty into the electromagnetic field. In order to visualize the quantum state of the light and its associated uncertainties, one can use the "ball on the stick" picture. In this picture, the quantum state of the optical field is represented by an arrow pointing from the origin to a location in a 2-dimensional plane where the x and y axes correspond to the amplitude and phase quadratures, respectively. The uncertainties in the quadrature operators is depicted by a ball of uncertainty around the arrowhead. As an illustrative example, the left image in Figure 1 displays a ball on the stick plot for a coherent state of light, which is the most classical quantum state of light and corresponds to the light produced by an ideal laser.

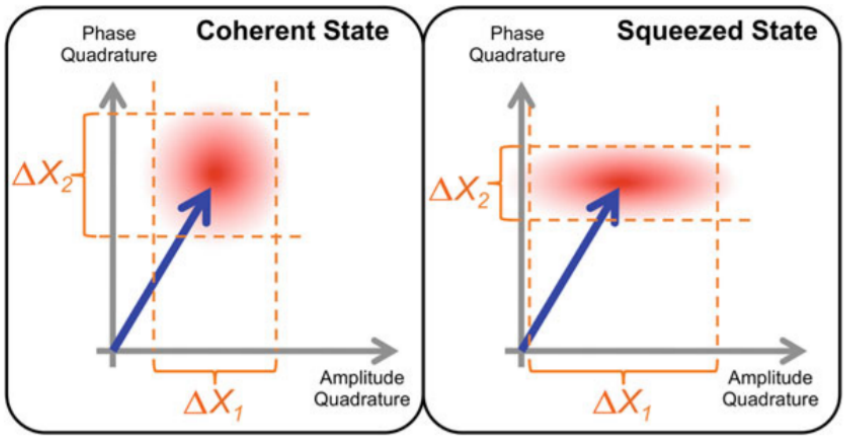

Figure 1: "Ball on the stick" plots for coherent light and phase squeezed light, obtained from [10].

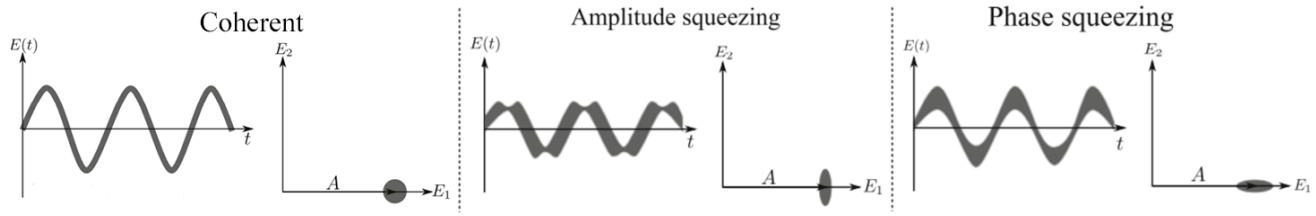

Figure 2: Electric fields and ball on the stick plots for coherent light, amplitude squeezed light, and phase squeezed light, all obtained from [5].

The finite uncertainty of the quadrature operators severely limits the ability to use classical light to discern subatomic length scales. This arises from the fact that one cannot perform accurate optical measurements when the electric field of the light is not known precisely. To counter this effect, one can use squeezed light instead of classical light in an interferometer setup. In squeezed states of light, the uncertainty of one quadrature operator is decreased while that of the other quadrature operator is simultaneously increased, such that the uncertainty principle is still satisfied. Squeezed light is known as phased squeezed or amplitude squeezed depending on whether the uncertainty of the amplitude quadrature or phase quadrature is decreased below its classical value. A ball on the stick plot of phase squeezed light is depicted in the right image of Figure 1. Although preparing squeezed light is a nontrivial process, it can be carried out using an optical parametric oscillator or other nonlinear optical devices. Distinct quantum states of light produce electric fields with different behaviors. Examples for three types of light are depicted graphically in Figure 2. From these images, it is evident that the uncertainty of the electric field of squeezed light does not behave like the corresponding uncertainty in coherent light, which is roughly classical light. In fact, at certain instants, the uncertainty of the electric field of the squeezed light decreases below that of coherent light. Thus, measurements using squeezed light that are performed at times when this uncertainty is lower than the classical value will be very accurate. These measurements are conducted using phase sensitive detection and provide a viable route to exceeding the SQL.

An optical technique, known as balanced homodyne detection, can be used to perform phase sensitive detection with squeezed light. A balanced homodyne detector (BHD) is composed of two photodiodes, a 50/50 beam splitter, and two sources of light: the signal and the local oscillator. An image of a BHD setup is displayed in Figure 3. The signal is the light that contains the desired information; for instance, it could be the light coming from the main interferometer that encodes the structure of a passing GW. On the other hand, the local oscillator is a stabilized source of light with its carrier frequency equal to that of the signal. In an interferometer, the local oscillator light can be obtained from the incident laser light before it reaches the main interferometer. In balanced homodyne detection, these two sources of light are first mixed by being sent through the beam splitter. Next, the two photodiodes measure the photocurrents induced by the two outgoing beams from the beam splitter. One can then measure and analyze these photocurrents, from which information about the quadratures can be extracted.

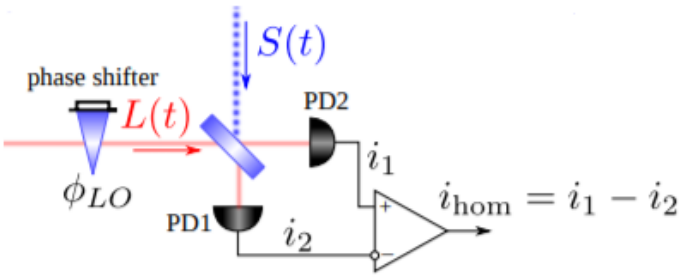

Figure 3: A standard BHD setup, obtained from [12].

Following the analysis presented in [12], we can describe this procedure mathematically. Let the electric fields of the signal and local oscillator light have quadratures $S_{c,s}(t)$ and $L_{c,s}(t)$, respectively, and carrier frequency ω:

$$S(t) = S_c(t)\cos(\omega t) + S_s(t)\sin(\omega t), \qquad L(t) = L_c(t)\cos(\omega t) + L_s(t)\sin(\omega t). \tag{3}$$

Due to inevitable quantum noise, the quadratures will contain terms due to noise. Denoting these by $n_{c,s}(t)$ and $l_{c,s}(t)$, respectively, the quadratures can be decomposed as

$$\begin{aligned} S_{c,s}(t) &= \text{signal} + \text{quantum noise} = G_{c,s}(t) + n_{c,s}(t) \\ L_{c,s}(t) &= \text{classical field} + \text{laser noise} = L^{(0)}_{c,s}(t) + l_{c,s}(t). \end{aligned} \tag{4}$$

Since the local oscillator is under the experimentalist's control, we will impose on it a phase shift, ϕ_{LO}, known as the homodyne angle: $L^{(0)}_c(t) = L_0\cos(\phi_{LO})$, $L^{(0)}_s(t) = L_0\sin(\phi_{LO})$. Such an alteration could be realized by changing the path length of the local oscillator. Additionally, we will assume that the local oscillator's amplitude is much greater than the other amplitudes in this scenario: $L_0 \gg G_{c,s}, n_{c,s}, l_{c,s}$. Under these assumptions, one can calculate the ideal photocurrents induced at the two photodiodes, which we denote by i_1 and i_2. In balanced homodyne readout, one chooses not to measure these currents, but instead measures the difference between them: $i_{\text{hom}} = i_1 - i_2$. To first order in $G_{c,s}, n_{c,s}$, and $l_{c,s}$, this is given by [12]

$$i_{\text{hom}} \propto L_0((G_c + n_c)\cos(\phi_{LO}) + (G_s + n_s)\sin(\phi_{LO})). \tag{5}$$

Evidently, this expression is independent of $l_{c,s}$, so the noise from the local oscillator does not factor into measurements of i_{hom}. In addition, Eq. (5) indicates that, by varying ϕ_{LO} and measuring i_{hom}, one can measure the signal's quadratures and linear combinations of them, with a precision limited only by the quantum noise of the signal.

In an interferometric GW detector, acquisition of the quadratures provides accurate information about the passing gravitational radiation. Thus, a properly constructed BHD presents the opportunity to probe exceptionally small length scales and improve GW detection. However, the real world is not so ideal. In the construction of a physical BHD, other sources of optical and electronic noise exist within the interferometer. The optical noise arises from noise present in the signal, and the electronic noise emerges from noise induced in the detector. For instance, an imperfect beam splitter will create an imbalance in the light beams emerging from it and introduce local oscillator noise into i_{hom}. In addition, this setup is susceptible to noise in its electronic circuits, such as thermal noise in the resistors and intrinsic $1/f$ noise. In order to analyze the noises within the electronic circuits, one must calculate the noise spectral density of each circuit element. Let the noise spectral density of the j^{th} circuit element be denoted by e_{n0j}. The exact form of e_{n0j} will differ for distinct circuit elements since their noise contributions will not be the same. Then, the noise voltage due to this element, denoted by E_{n0j}, is obtained via

$$E^2_{n0j} = \int_0^\infty df\ |e_{n0j}|^2. \tag{6}$$

Generally, this integral will be limited by the finite bandwidth over which the circuit operates. Finally, the total noise voltage due to all the circuit elements, denoted by E_{n0}, can be

obtained from an RMS summation:

$$E_{n0}^2 = \sum_j E_{n0j}^2. \tag{7}$$

Proper analyses of all of these noises must be incorporated in order to correctly interpret the data from a BHD.

Current gravitational wave observatories do not exploit balanced homodyne detection of this sort. Instead, these experiments primarily use DC readout [11], in which a single photodetector measures the light output from the main interferometer's beam splitter. As shown in [12], DC readout schemes are affected by the noise in the local oscillator, unlike ideal balanced homodyne readout. In addition, DC readout schemes are not as effective as balanced homodyne readout at measuring arbitrary quadratures of light in an interferometer. This is best done by using squeezed light and a BHD with a variable homodyne angle, which enables one to take advantage of the reduced quadrature uncertainties of the squeezed light. Therefore, it is believed that balanced homodyne detection will provide more precise interferometric measurements in GW detectors than the current DC readout schemes do. We hope that further research into this technology will lead to the implementation of balanced homodyne detectors in GW interferometers and improved detection of gravitational radiation.

2 Objective

The goal of this project will be to construct a balanced homodyne detector. Once completed, we will then analyze the electronic and optical noise that exists within the BHD.

3 Approach

The BHD will be constructed from standard optical devices used in interferometry, including a laser, beam splitters, and photodiode detectors. More specifically, we will use InGaAs photodiodes. These are optimal for this setup because they have a high quantum efficiency and convert incident light into photocurrent very effectively. To amplify the interferometric signal and convert it from a current signal to a voltage signal, we will implement transimpedance amplifiers with low current noise. The specific transimpedance amplifiers to be used are homemade ones from the Adhikari lab, and it is desired that they contribute a minimal level of electronic noise. An image of a sample transimpedance amplifier circuit, which will be used as a guide in the BHD construction, is displayed in Figure 4.

Moreover, in order to analyze the optical and electronic noise in these devices, we will utilize two programs known as LISO and Finesse. LISO will be used to optimize electronic noise, and Finesse will be used to simulate the noise in the interferometer. Proper application of both programs is central to gauging the success of the final homodyne detector. Lastly, when a mathematical analysis of the noise in the BHD is required, Python Jupyter notebooks will be used to carry out analytic calculations and plot results.

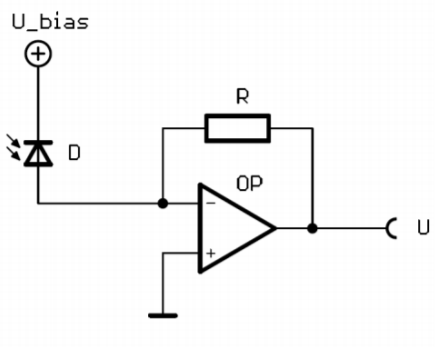

Figure 4: A basic transimpedance amplifier circuit, obtained from [4]. This circuit contains a photodiode (D), a resistor (R), and an operational amplifier (OP). U_bias and U denote the bias and output voltages, respectively.

4 Timeline

Given the period of 10 weeks to achieve these goals, my tentative work plan is as follows:

Work Plan	
Week(s)	Tasks
1	Become acquainted with important software, equipment, and laboratory protocol.
2-9	Construct the BHD and analyze its noise (will be done simultaneously).
9-10	Prepare final report and presentation.

Finally, I will also take into consideration the various SURF requirements and their deadlines, which include two interim reports, an abstract, a final report, and a final presentation.

References

[1] A. I. Lvovsky, *Squeezed Light*. ArXiv e-prints (2016), arXiv:1401.4118v2 [quant-ph].

[2] B.P. Abbott et al., *Observation of Gravitational Waves from a Binary Black Hole Merger*. Phys. Rev. Lett. **116**, 061102 (2016).

[3] C. W. Misner, K. S. Thorne, and J. A. Wheeler, *Gravitation*. (1973).

[4] H. Grote, et. al., *High power and ultra-low-noise photodetector for squeezed-light enhanced gravitational wave detectors*. Opt. Express, **24**, 20107-20118 (2016).

[5] H. Miao, *Exploring Macroscopic Quantum Mechanics in Optomechanical Devices*. (2012).

[6] H. W. Ott, *Noise Reduction Techniques in Electronic Systems*. (1988).

[7] J. G. Graeme, *Photodiode Amplifiers: Op Amp Solutions*. (1995).

[8] K. Thorne, *Ph237b: Gravitational Waves*. California Institute of Technology (2002).

[9] https://www.ligo.caltech.edu/

[10] M. Bassan, et. al, *Advanced Interferometers and the Search for Gravitational Waves*. (2014).

[11] K. Nakamura and M. Fujimoto *Double balanced homodyne detection*. ArXiv e-prints (2018), arXiv:1711.03713v2 [quant-ph].

[12] S. L. Danilishin and F. Y. Khalili, *Quantum Measurement Theory in Gravitational-Wave Detectors*. ArXiv e-prints (2012), arXiv:1203.1706v2 [quant-ph].

[13] S. M. Carroll, *Spacetime and Geometry: An Introduction to General Relativity*. (2004).

[14] W. Ketterle, *8.422 Atomic and Optical Physics II*. Spring 2013. Massachusetts Institute of Technology: MIT OpenCourseWare, https://ocw.mit.edu. License: Creative Commons BY-NC-SA.